International Journal of Fatigue 145 (2021) 106084

Contents lists available at ScienceDirect

International Journal of Fatigue

journal homepage: www.elsevier.com/locate/ijfatigue

Fatigue characterization of polyethylene under mixed mode I/III conditions

Anja Gosch [a], Florian J. Arbeiter [a,*], Michael Berer [b], Tomáš Vojtek [c,d], Pavel Hutař [c], Gerald Pinter [a,b]

[a] Materials Science and Testing of Polymers, Montanuniversitaet Leoben, Otto-Gloeckel-Str. 2, 8700 Leoben, Austria
[b] Polymer Competence Center Leoben GmbH, Roseggerstr. 12, 8700 Leoben, Austria
[c] Institute of Physics of Materials, Academy of Sciences of the Czech Republic, Žižkova 22, 616 62 Brno, Czech Republic
[d] Central European Institute of Technology (CEITEC), Brno University of Technology, Purkyňova 123, 612 00 Brno, Czech Republic

ARTICLE INFO

Keywords:
Mixed Mode I/III fatigue loading
Polyethylene
Fracture surface analysis
Equivalent stress intensity factor
Polymer

ABSTRACT

Mixed mode I/III fatigue fracture behaviour of bulk polymers is scarcely investigated. Thus, the aim of this work is to focus on the comparison of pure mode I and mixed mode I/III fatigue loading of polyethylene. During mixed mode I/III testing, both increases and decreases of lifetime were observed, depending on the levels of applied mode I and mode III loading. Additionally, the critical influence of friction and the accompanying increase of local temperature between the shear loaded crack flanks in mode III, as well as the dominant fracture mechanisms were discussed based on the fracture surface morphology.

1. Introduction

Mixed mode loading mechanisms in bulk polymers are rarely investigated, even though a significant amount of mixed mode loading close to the crack tip is likely to occur in several applications, such as randomly orientated cracks in a component which is used in rolling contact [1–5], twisting of a pipe during installation, etc. Therefore, it can be beneficial to possess detailed knowledge about mixed mode crack growth behaviour of polymers as shown in previous investigations [6]. For component design, the long-time performance of a polymer part can be evaluated via fatigue testing, which is usually performed only in mode I (tensile loading). However, mixed mode crack growth (in plane shear loading defined as mode II and out of plane shear loading as mode III) can display completely different crack growth behaviour and mechanisms. This is due to the complex nature of mixed mode crack growth, in which the crack flanks are closed during testing, which in turn can cause friction and wear abrasion and the effect of so called "mode I branching". The latter mechanism is responsible for a change in the crack growth direction, where the local loading situation changes from mode II or mode III into mode I. This is commonly found in mixed mode loading tests on metals [7–9]. Furthermore, mixed mode crack propagation is known as non-self-similar, which means cracks change their direction during mixed mode loading [10].

As stated above, understanding mixed mode fatigue crack growth can provide additional information with regard to component design, as shown in previous research [2,11]. This makes the topic highly interesting to gain more information about the behaviour of components in complex loading situations. In a recent study [12], mixed mode I/III fatigue loading was applied to cracked round bar specimens (CRB) of a polyoxymethylene homopolymer (POM-H) and the resulting fatigue fracture curve was compared to pure mode I fatigue tests. The work also presented an equivalent stress intensity factor (K_{eq}) concept, which can take both loading cases of mode I and mode III into account. Nevertheless, some open questions concerning the crack growth mechanisms during mixed mode loading remain due to the rather difficult fracture behaviour of POM-H. To better understand the complex mixed mode loading situation and the subsequent fracture behaviour of polymers, a study on a well-known reference material seems indispensable. Therefore, the mixed mode I/III fatigue fracture behaviour of high-density polyethylene (PE), which is well investigated for mode I, was characterized in the present study. PE is a commercially available polymer, which is used in daily applications (packaging, bottles, etc.) and technical components (gas or water pipes, tanks, etc.). Due to the increasing requirements in engineering applications, such as pressure piping, its fatigue behaviour in mode I is well characterized for the estimation of the life-time performance [13–19]. Furthermore, the occurring fracture mechanisms are well documented via optical methods (light-microscope and SEM analysis of the fracture surface) and are available as reference for the mixed mode testing.

* Corresponding author.
E-mail address: florian.arbeiter@unileoben.ac.at (F.J. Arbeiter).

https://doi.org/10.1016/j.ijfatigue.2020.106084
Received 18 August 2020; Received in revised form 1 December 2020; Accepted 2 December 2020
Available online 15 December 2020

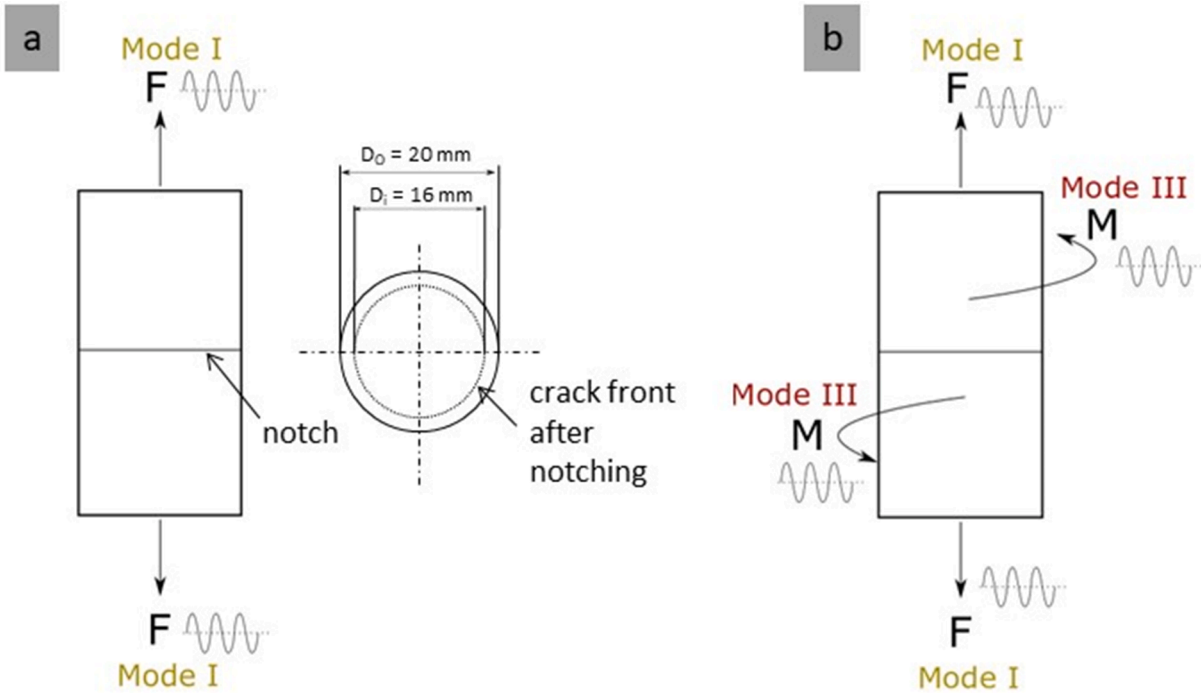

Fig. 1. Loading conditions of the PE - CRB specimens used in this work – (a) Mode I crack opening conditions realized as tensile fatigue load (b) Mixed mode I/III crack opening conditions realized as combined tensile and torsional fatigue load (adapted from [12]).

Table 1
Details and parameters of the fatigue test series conducted on PE specimens in mode I and mixed mode I/III (tensile load F, torsional moment M and stress intensity factor in mode I K_I and mode III K_{III}).

	Mode I	Mixed Mode I/III (combined Mode I and Mode III loading)
Servo hydraulic testing machine	MTS 858 Axial Torsional (MTS Systems GmbH, Minnesota, USA)	MTS 858 Axial Torsional (MTS Systems GmbH, Minnesota, USA)
Frequency	10 Hz	5 Hz
R-ratio	0.1	0.1 (for both loading cases)
Examined F regime (max. value)	2200–3100 N	2300–2600 N
Resulting K_I regime (max. K_I)	0.6–0.9 MPa $m^{1/2}$	0.6–0.8 MPa $m^{1/2}$
Examined M regime (max. value)	–	5–10 Nm
Resulting K_{III} regime (max. K_{III})	–	0.3–0.6 MPa $m^{1/2}$
Clamping distance	35 mm	35 mm
Data acquisition	Peak/valley data every 100 cycles Hysteretic data every 1000 cycles	Peak/valley data every 100 cycles Hysteretic data every 1000 cycles

2. Materials and methods

2.1. Material

The used material in this work was a high-density polyethylene pipe grade material with high resistance against crack growth and a density of 0.95 kg/dm^3 (supplied as PE100-RC, extruded rods with a diameter of 20 mm, AGRU Bad Hall, Austria). To characterize the melting temperature and degree of crystallinity of the material, differential scanning calorimetry (DSC) measurements were performed according to ISO 11357-1:2016 (heating rate $\Delta T/\Delta t = 10$ K min^{-1}, testing atmosphere N_2 50 mL min^{-1}, temperature range 0–160 °C, 2 tested samples) on a DSC 1 (Mettler Toledo Schwarzenbach, CH). The investigated PE type has a melting temperature of 130 ± 1 °C and a degree of crystallinity of 64 ± 1.4%. Both values were determined at the first heating run. For the calculation of the degree of crystallinity the specific heat of fusion of a 100% crystalline PE, which is 290.0 J/g according to [20], was used.

2.2. Experimental

The experimental procedure used in this work was similar to a recently published paper dealing with the mixed mode I/III fatigue behaviour of POM-H [12]. However, to improve the readability, this section repeats the crucial details and parameters concerning the conducted experiments and data analysis.

The specimen type used for fatigue testing was the CRB specimen, for which the exact dimensions are shown in Fig. 1. A sharp circumferential notch was introduced with a razor blade (blade thickness 0.1 mm, tip radius <5 μm) by mounting the specimens on a lathe. The notching depth was approximately 2 mm (10% of the initial diameter) for all specimens examined (following a recently published standard for PE [21]).

The CRB specimens were loaded in two different ways: (1) pure mode I tensile fatigue loading according to Fig. 1a and (2) mixed mode I/III through a combined tensile and torsional fatigue load as shown in Fig. 1b. All experimental details and testing conditions are summarized in Table 1., one can recognize a difference in frequency for the pure mode I and the mixed-mode I/III fatigue tests. This change for mixed-mode tests was due to technical limitations arising from the testing machine. However, published work shows, that this should have no influence on the results within the applied frequency range [22].

An optical microscope “SZX12” from Olympus (Olympus Life Science Europe GmbH, Hamburg, Germany), as well as a scanning electron microscope “Vega II” from TeScan (Tescan Orsay Holding, a. s., Brno, Czech Republic) were used for the detailed fracture surface analysis.

To investigate the formation and the path of growing cracks in mixed mode loading, so called “crack freezing” experiments were conducted

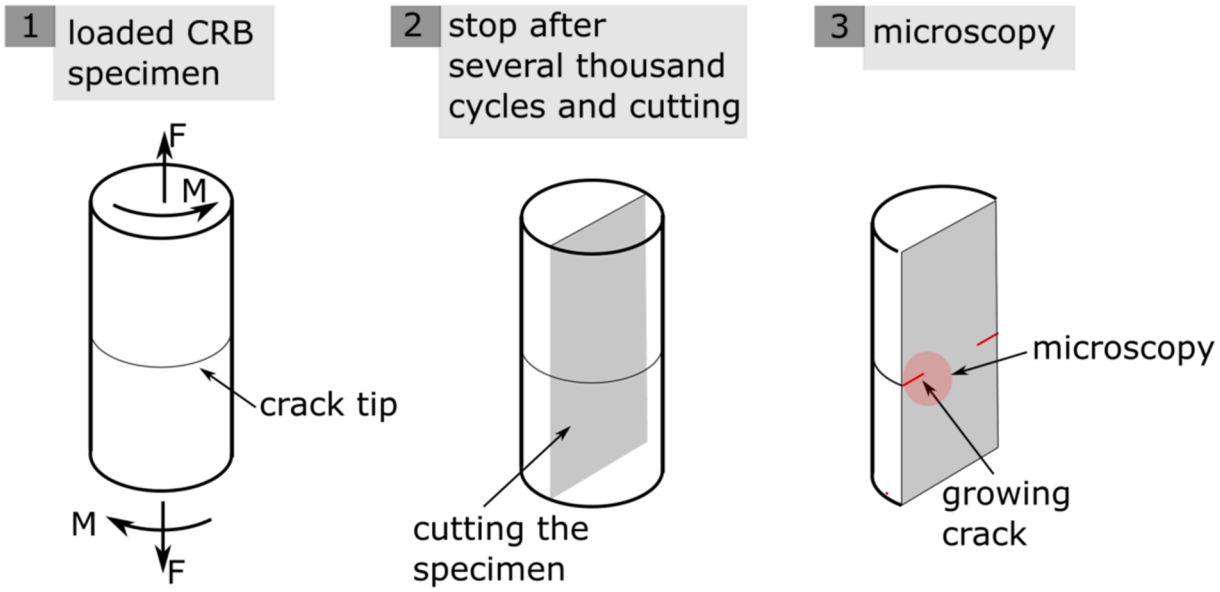

Fig. 2. Procedure for the "crack freezing" experiments: (1) Mixed mode loaded specimen with sharp notch; (2) test stopped after several thousand cycles before the complete fracture occurred and cut of the specimen; (3) Light-microscopy and SEM analysis of the crack extension (marked red). (For interpretation of the references to colour in this figure legend, the reader is referred to the web version of this article.)

Table 2
Equations to calculate the initial stress intensity factor range in mode I (ΔK_I) according to [21,23].

$\Delta K_I = \frac{\Delta F}{\pi b^2}\sqrt{\frac{\pi a_0 b}{1000 r}} f_1\left(\frac{b}{r}\right)$	(1)
$b = r - a_0$	(2)
$f_1\left(\frac{b}{r}\right) = \frac{1}{2}\left[1 + \frac{1}{2}\left(\frac{b}{r}\right) + \frac{3}{8}\left(\frac{b}{r}\right)^2 - 0.363\left(\frac{b}{r}\right)^3 + 0.731\left(\frac{b}{r}\right)^4\right]$	(3)

Table 3
Equations to calculate the initial stress intensity factor range in mode III (ΔK_{III}) according to [24].

$\Delta K_{III} = \Delta\tau\sqrt{\pi b} f_3\left(\frac{b}{r}\right)$	(4)
$\tau = \frac{2T}{\pi b^3}$	(5)
$f_3\left(\frac{b}{r}\right) = \frac{3\sqrt{1 - b/r}}{8}\left\{1 + \frac{1}{2}\frac{b}{r} + \frac{3}{8}\left(\frac{b}{r}\right)^2 + \frac{5}{16}\left(\frac{b}{r}\right)^3 + \frac{35}{128}\left(\frac{b}{r}\right)^4 + 0.208\left(\frac{b}{r}\right)^5\right\}$	(6)

(schematically shown in Fig. 2), before the complete fracture of the tested specimens. Experiments were stopped after several thousand cycles (close to the final failure), the specimens were cut along their longitudinal axis and the crack tip was investigated via microtome slices (light microscope) and SEM images.

2.3. Expression of the mixed mode crack driving force using the equivalent stress intensity factor

The initial stress intensity factor range ΔK in mode I and mixed mode I/III was determined according to the corresponding equations given in Table 2 and Table 3.

In this equations ΔF is the difference between the minimum and maximum load, r the outer radius of the specimen, a_0 the initial crack length, b the ligament radius and $f_1(b/r)$ a geometry dependent factor typical for the CRB specimen in mode I [21,23].

In these equations τ is the shear stress, T is the torsional moment, Δτ and ΔT are the differences between the minimum and maximum values of shear stress and torsional moment, respectively; b is again the ligament radius after notching, $f_3(b/r)$ is the geometry dependent factor for the CRB specimen in mode III and r the outer radius of the bar [24].

Furthermore, a so called "equivalent stress intensity factor" (K_{eq}) was calculated similar to our previous publication [12]. The parameter K_{eq} is able to combine stress intensity factors in different loading modes into a single value. The easiest expression for K_{eq} is based on the energy release rate (G) for brittle fracture. It is given by Eq. (7) for plane strain conditions [25]:

$$K_{eq} = \sqrt{K_I^2 + K_{II}^2 + \frac{1}{1-\nu}K_{III}^2} \tag{7}$$

where ν is the Poisson's ratio. It should be mentioned at this point, that there are several equations for mixed mode loading and K_{eq} available in literature, e.g. in [7,26–28], based on different assumptions and/or boundary conditions. Under cyclic loading, the equivalent stress intensity factor range ΔK_{eq} is used instead of K_{eq}. The influence of mode II (K_{II}) is completely eliminated for the CRB specimen geometry used in the present study. This was verified via numerical simulations. Furthermore, the coefficient $1/(1-\nu)$ in Eq. (7) is expected to be smaller in reality, since mode III crack propagation is less efficient compared to the other loading modes. This aspect was also found in previous research for fatigue cracks in metallic materials [29] and for polymers [12]. Hence, a representative parameter λ was defined and ΔK_{eq} can be simplified for mixed mode I and mode III as shown in Eq. (10):

$$\Delta K_{eq} = \sqrt{\Delta K_I^2 + \lambda \Delta K_{III}^2} \tag{8}$$

According to [28,30], the values used for λ are typically between 0.9 and 1.2 for metallic materials. For POM-H, a value of 1 was used as a first step in [12] for the stress ratio of R = 0.1. For PE, the parameter λ is initially unknown. Therefore, the value of 1 was also used in a first step:

$$\Delta K_{eq} = \sqrt{\Delta K_I^2 + \Delta K_{III}^2} \tag{9}$$

Additionally, it is stated in literature that also the ratio of the applied mode I and mode III levels ($\Delta K_{III}/\Delta K_I$) influence the fatigue behaviour. Therefore, the parameter ΔK_{eq} can provide a much better fit of the experimental data, when this ratio is also included in the calculation. In [12] a new equation for ΔK_{eq} was proposed and successfully implemented for POM-H:

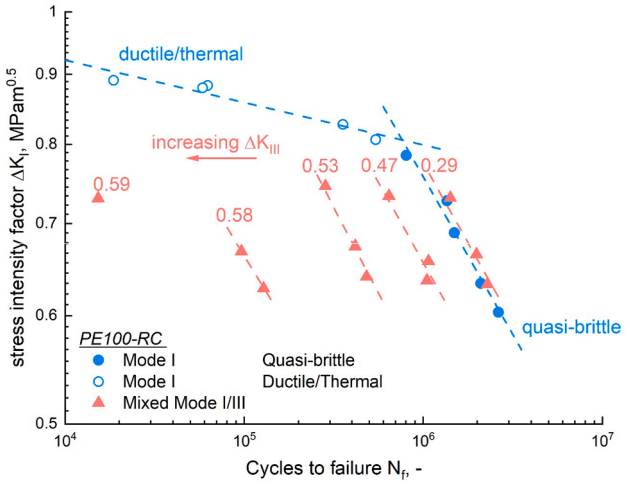

Fig. 3. Fatigue fracture behaviour of PE evaluated in pure mode I and mixed mode I/III fatigue testing: an increasing mode III amount (caption of mixed mode I/III data points is the mean value of ΔK_{III}) leads to a decrease in the cycles to fracture.

$$\Delta K_{eq} = \sqrt{\Delta K_I^2 + 0.9\left(\frac{\Delta K_{III}}{\Delta K_I}\right)\Delta K_{III}^2} \quad \text{(valid for } \frac{\Delta K_{III}}{\Delta K_I} < 1.0\text{)} \tag{10}$$

3. Results and discussion

3.1. Mode I and mixed mode I/III fatigue behaviour of PE

To determine the influence of mixed mode I/III loading conditions on fatigue testing of PE, pure mode I tests were conducted to establish a benchmark of the material. The resulting mode I fracture curve (stress intensity factor range ΔK_I versus the cycles to failure N_f) is shown in Fig. 3.

In the current study, N_f was used for all presented figures. Usually, N_f can be separated into a crack initiation part (cycles to crack initiation $N_{initiation}$) and a crack propagation part (cycles during crack propagation $N_{propagation}$). The characterization of $N_{initiation}$ is often done by evaluation of the cyclic compliance of the specimen. For this, it is necessary to apply local strain sensors (e.g. clip on extensometers, placed in a circle around the specimen). In the case of mode I in PE-HD this has been done many times before as shown in literature [31,32]. However, in the present work it was not possible to calculate $N_{initiation}$, since the mixed mode I/III loading situation requires a very complex biaxial measuring equipment. Subsequently, the compliance value documented by the testing machine itself (without the use of local extensometers) is too coarse for any detailed analysis of the mixed mode I/III crack growth behaviour (an example of this is shown in the Appendix A). Therefore, it is not reliably possible to determine the initiation point, or subsequently the evaluation of the crack growth kinetics curve based on the compliance data, which would be very desirable for further analysis and transferability to other components.

Looking at the results of the fracture curve, as expected from results in literature [14–19,33–35], two regions can be detected in the mode I fatigue curve:

(1) the ductile/thermally controlled region, in which high ΔK_I values lead to a significant decrease in N_f, which is often accompanied by a significant amount of hysteretic heating and large-scale ductile deformation of the material. This behaviour was also observed for the investigated material in the present study.
(2) the quasi-brittle region, at rather low values of ΔK_I and high corresponding values of N_f, in which the fracture surface appears rather brittle on a macroscopic scale, but shows signs of fibrillation on a microscopic level. This type of failure in PE is a rather complex process, consisting of void initiation at the crack tip, void growth and coalescence, craze formation and finally crack growth [32,36]. Contrary to (1) the deformation process is very localized in a very small area in front of the crack tip, allowing also for the application of linear elastic fracture mechanics [37–42]. For PE it was found, that the process is subsequently mostly governed by molecular disentanglement in the stretched craze fibrils [32,43–45].

Subsequently, mixed mode I/III tests were performed and the results added to Fig. 3 (caption is ΔK_{III}). Generally, when an additional loading mode is applied to pure mode I, a decrease in the measured life-time is expected, which was confirmed by most data shown in Fig. 3. It is worth noting that for low amounts of ΔK_{III} (around 0.3 MPam$^{1/2}$) no decrease in N_f was found, whereas, for higher amounts ($\Delta K_{III} \geq 0.5$ MPam$^{1/2}$) a significant decrease in N_f occurred. Interestingly, a similar slope of the mixed-mode I/III failure curves and the mode I quasi-brittle curve can be observed. This indicates, that additional loading in mode III, produces a

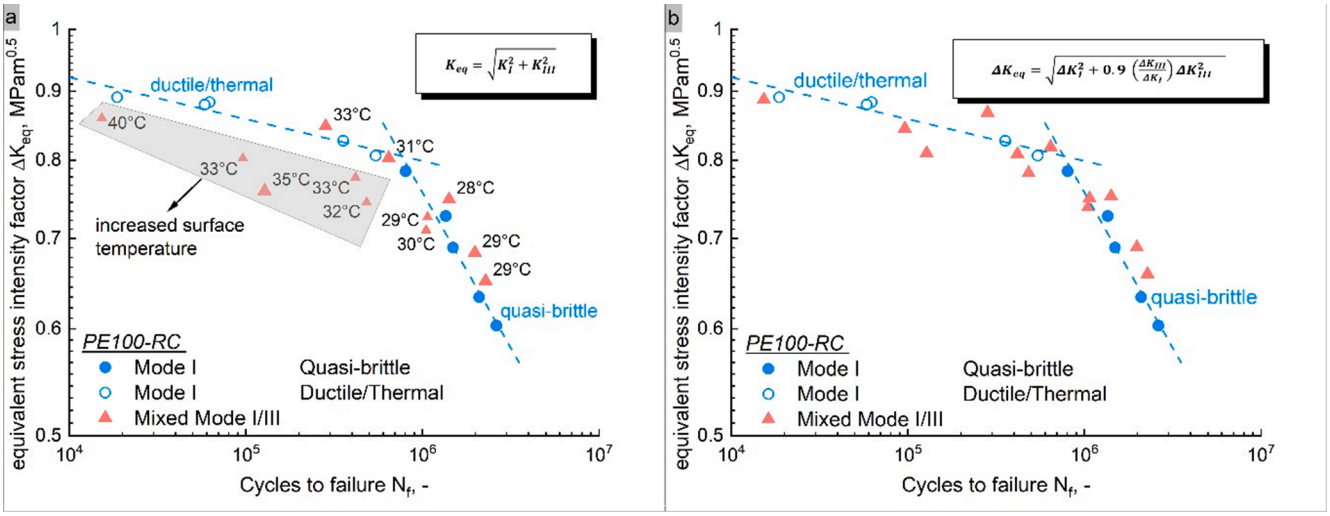

Fig. 4. Fatigue behaviour of pure mode I and mixed mode I/III loaded PE represented via the equivalent stress intensity factor ΔK_{eq}: (a) ΔK_{eq} calculated via Eq. (9), where the caption of mixed mode data points is the measured surface temperature during testing and (b) ΔK_{eq} calculated via Eq. (10), where the mode III/mode I ratio is taken into account.

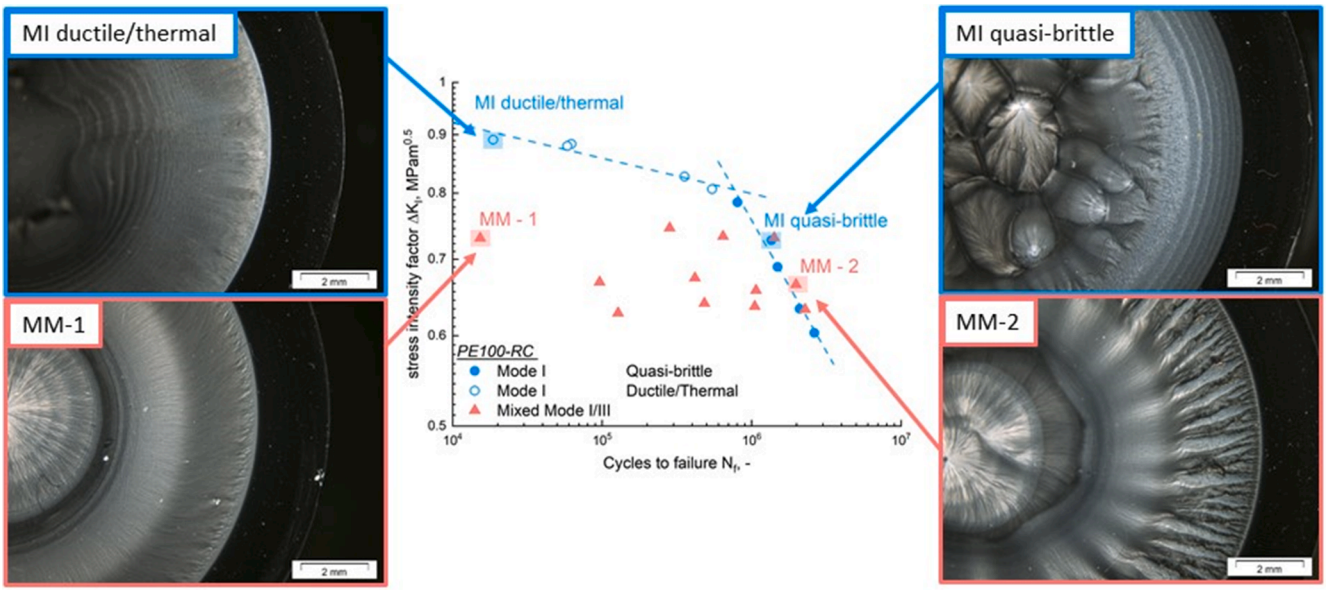

Fig. 5. Light microscope pictures of fracture surfaces in different parts of the fatigue fracture curve of PE: mode I loading ("MI ductile/thermal" and "MI quasi-brittle") and mixed mode I/III loading ("MM-1" with high ΔK_{III} loading and "MM-2" with low ΔK_{III} loading).

similar trend between the applied loading and resulting cycles to failure, only shifted to lower values of N_f.

For a better comparison, it is of high interest to compare both loading cases via a representative parameter, which simultaneously takes mode I and mode III loading into account. This concept is based on the assumption that an absolute value, which is the sum of two loading cases, is able to fully characterize the fatigue crack growth of mixed mode I/III loading [10]. Previous investigations on POM-H showed promising results by using the equivalent stress intensity factor ΔK_{eq}, as defined in Eqs. (8) to (10) [12].

3.2. Equivalent stress intensity factor ΔK_{eq}

The use of ΔK_{eq} allows the combination of both loading cases and provides information about the partial contribution of pure mode I and mixed mode I/III loading. In the case of pure mode I, ΔK_{eq} is identical to ΔK_I. For mixed mode I/III specimens, the amount of ΔK_{eq} can be calculated using various equations proposed in literature [10]. As a starting point in this study, the interactions of mode I and mode III were neglected and it was assumed that both loading cases are affecting the results equally (Eq. (9)). Fig. 4-a displays the resulting fatigue fracture curve based on ΔK_{eq} calculated from Eq. (9) in addition with the maximum specimen surface temperature measured during the testing of the mixed mode I/III data points.

The evaluated data points from pure mode I and mixed mode I/III loading almost coincided with the application of ΔK_{eq} (calculated via Eq. (9)) in the area of low to moderate levels of ΔK_{III}. This indicates, that both loading cases contribute with a similar efficiency regarding the fatigue resistance of the material in the region of quasi-brittle fatigue crack growth. Interestingly, the specimens tested with the lowest amount of ΔK_{III} appear to be even slightly shifted towards higher life-times. At higher applied levels of pure mode I and mixed mode I/III, in the region of "hysteretic heating-induced thermal failure" [38], samples showed an increased surface temperature (up to 40 °C for the highest amount of ΔK_{III}). This is especially critical, since mechanical properties of polymers are highly sensitive to temperature and an increase in temperature can significantly change the life-time of the tests [12,46–48]. However, hysteretic heating should not significantly affect the region of quasi-brittle failure, since it was found that in this regime, the temperature increase in PE-HD is usually rather low (~2 to 4 K) and stabilizes after a few thousand cycles. This was also measured in prior work via temperature sensors inside of the specimen, close to the crack tip itself [22].

Contrary to the results in the quasi-brittle region, tests at high levels of additional ΔK_{III} did not collapse onto the pure mode I results of the ductile/thermally controlled region by using Eq. (9). This indicates, that another contributing factor, besides mode I and mode III loading, as well as classical hysteretic heating, appears to be present. Based on the boundary conditions of the test setup and knowledge from previous research, this additional factor is most likely friction and wear abrasion [12]. Hence, the use of Eq. (9) appears to be a useful tool to identify loading conditions, which are significantly influenced by friction and wear abrasion of the crack flanks.

As shown in our previous research [12], it is possible to also consider friction and abrasion in ΔK_{eq} by including a ratio of $\Delta K_{III}/\Delta K_I$, as shown in Eq. (10). The results of using this equation are presented in Fig. 4-b. The data points of both loading cases coincide well, which means that the mode III/mode I ratio, which is also responsible for the amount friction and abrasion during the test, influences the mixed mode I/III fatigue behaviour of PE significantly. The application of the adapted ΔK_{eq} equation (Eq. (10)) enables the explicit description of the relationship between applied loading and subsequent cycles to failure over the whole testing range. Based on the good correlation of the two loading cases, the adapted version of ΔK_{eq} according to Eq. (10) is expected to be usable for life-time prediction of mixed mode I/III loaded PE components.

3.3. Detailed fracture surfaces analysis

To gain more information about the fracture process during fatigue testing, it is common to investigate the fracture surfaces in detail via light microscopy and SEM analysis. Generally, the crack growth mechanisms observed on the fracture surface of a mode I loaded PE specimen are a series of complex processes involving cavitation, voiding, coarse fibril formation and rupture [49], which is commonly termed "crazing". Adding a further loading case (mode III) leads to even more complex shapes on the fracture surfaces, which can be difficult to interpret as shown in the next chapter.

3.3.1. Fracture surface - Macroscopic level

In this section, an optical analysis of PE fracture surfaces is presented. To provide a rough overview, fracture surfaces of both loading

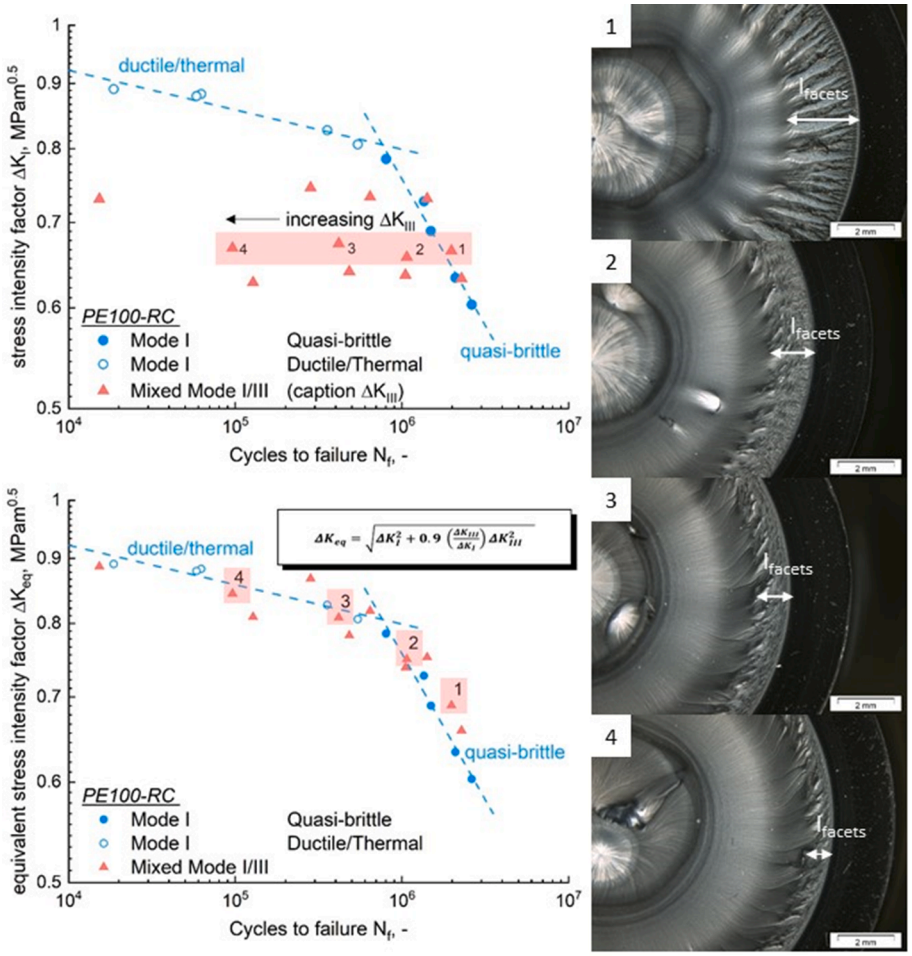

Fig. 6. Increasing mode III loading leads to a decrease in the facet length l_{facets} on the fracture surface of mixed mode I/III loaded PE specimens (for all investigated specimens, a similar mode I loading level was used during the tests).

cases in pure mode I and mixed mode I/III are compared in Fig. 5. Representative specimens from the ductile/thermal and quasi-brittle region of the mode I loaded specimens were chosen for a detailed optical analysis: "MI ductile/thermal" and "MI quasi brittle". In the case of the mixed mode I/III loading two specimens with different amounts of mode III were chosen for the fracture surface investigations: "MM-1" was loaded with a very high amount of ΔK_{III} and "MM-2" was loaded with a low amount of ΔK_{III}.

The fracture surface of the ductile/thermal failure is shown in Fig. 5 ("MI ductile/thermal"), where high amounts of ΔK_I lead to relatively short cycles to failure. "MI ductile/thermal" specimens display large scale tearing on the fracture surface and the microscopic texture displays a rather smooth appearance, which was also found in literature for PE [33,50–52]. In the region of quasi-brittle failure, the fracture surfaces show a similar appearance as found in previous research [49–53]: Directly after the initial notch, the fracture surface displays indications of blunting and step wise discontinuous crack growth, detected as lines on the fracture surface. Discontinuous crack growth in polymers is caused by two mechanisms taking place at the same time: crazing and micro shear banding. The competition between these two crack growth mechanisms causes forward steps in the crack growth, which are known as discontinuous crack growth (DCG) bands [14,50,53]. The last state during a fatigue test of the "MI quasi-brittle" specimen displays indications of plastic flow towards the middle of the specimen and is the result of high loads and a ductile fracture of the remaining ligament.

The investigated material displays also a macroscopically flat fracture surface (crack growth in the initial crack plane) for all mixed mode I/III loaded specimens, which is in agreement with literature for this type of specimen [10,54–57]. In the presence of mixed mode I/III loading, the area close to the initial crack tip is especially interesting. This area is highly influenced by mixed mode forces, which can lead to formations, significantly different from pure mode I loading, on the fracture surface. Macroscopically, these formations can be oriented in radial direction (compare "MM-2") or have a smeared-out appearance (compare "MM-1"). The fracture surface of "MM-1" appears smooth and "smeared out" with signs of abrasion between the crack flanks. At low amounts of mode III loading, the "MM-2" displays large radial formations close to the initial crack tip, which are called "factory roof" formations [12,28,29,55,56]. Factory roof formations are mixed mode facet formations occurring directly after the crack initiation phase with a 45° sloping "roof". This is the result of cracks, trying to propagate in local mode I by twisting the crack plane. Similar formations, although not as pronounced, were also found in previous research on polyoxymethylene [12]. The appearance of factory roof formations can lead to crack closure effects during testing, which is commonly known from metals [8,28,58–61]. This effect, which is also called "roughness induced" crack closure, is caused by the misfit of a microscopically rough fracture surface. During this state the crack is closed as a result of the contact between the fracture surfaces. Subsequently, the crack cannot propagate and the acting driving force is hindered, which can influence the measured cycles to failure. In this work, a slight increase in the measured life-time of mixed mode I/III specimens with low amounts of mode III loading compared to the pure mode I loaded specimens was detected (compare "MM-2" in Fig. 5). The measured cycles to failure

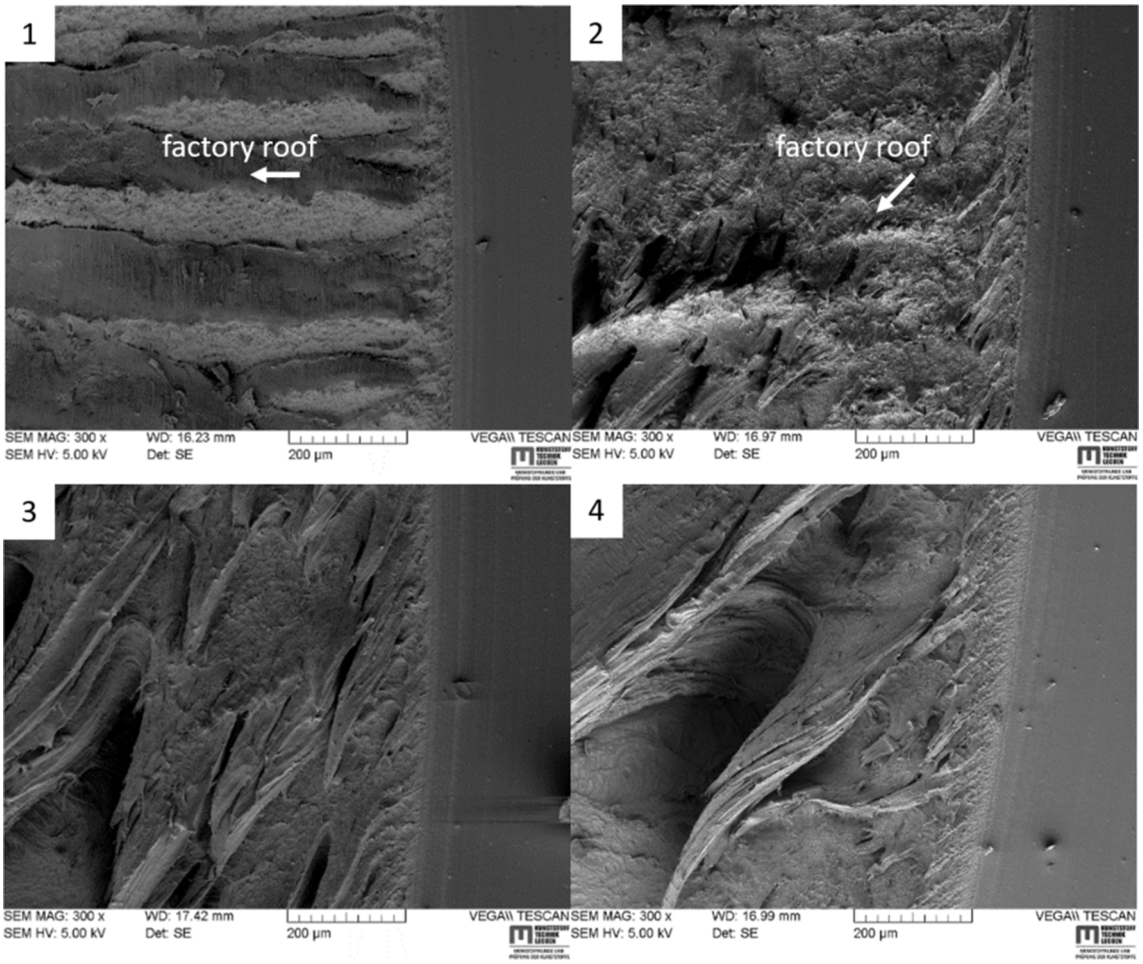

Fig. 7. SEM images from the fracture surfaces in Fig. 6 with a magnified view on the crack growth initiation area close to the notch tip show a change in the direction of the factory roof formations with increasing mode III loading.

slightly increase in comparison to the pure mode I loaded samples, even though an additional loading case (mode III) was applied. This could be an indication of a crack closure effect in the regime of low mode III loading amplitudes. The factory roof formations on the "MM-2" surface disappear after around 2 mm of crack growth, where the mechanism changes from mixed mode I/III loading to the final fracture (close to the specimen centre).

Based on the findings regarding the overall differences in fracture surface appearances, a more detailed analysis of the exact influence of the applied mixed mode I/III ratio is the logical next step. To discuss the influence of an increasing mode III amount on the appearance of the fracture surface, specimens at the same level of mode I but with increasing mode III loading were investigated and compared.

3.3.2. Influence of increasing mode III level on the fracture surface appearance

The influence of an increasing mode III amount on the fracture surface appearance of mixed mode I/III loaded PE specimens (nearly constant mode I loading) is presented in Fig. 6. Both variations of plotting the results with the applied ΔK_I value, as well as the ΔK_{eq} on the ordinate are presented.

The specimen with the lowest amounts of mode III displays the characteristic and aforementioned factory roof formations close to the notch tip, as shown in Fig. 6-(1). The factory roof formations display no indications of friction and wear abrasion on a macroscopical level. This argument is strengthened also by the fatigue fracture curve, where no decrease in life-time was measured compared to the pure mode I loaded specimens. Contrary to expectations, the additional loading in mode III induces a slight increase of the life-time (as discussed in the previous section with the crack closure effect). With an increasing level of mode III (see specimen (2) and Fig. 6) the area on the fracture surface, where the typical factory roof formations are visible, decreases and the overall appearance of the area changes slightly. In the graph showing ΔK_{eq}, the specimens fall onto the line of the quasi-brittle failure in pure mode I. This might indicate, that no crack closure effect is present, but the applied amount of mode III also does not yet lead to significant abrasion and hysteretic heating, which would change the failure mode from quasi-brittle to thermally induced ductile failure. Further increases in mode III (specimens marked (3) and (4)) lead to an even smaller area of mixed mode indications, where in specimen (1) factory roof formations are visible. Furthermore, the structures in this area change the direction into a more tangential direction, which is in agreement with previous literature [54–56].

To get a better understanding of the exact formations in the first area close to the initial notch, a detailed investigation via SEM is shown for specimens (1) to (4) in Fig. 7. In the first picture (Fig. 7-(1)) the factory roof formations display no sign of deformation and the direction of the factory roof is pointed directly towards the specimen centre. For specimen (2), the area close to the crack growth initiation appears flatter and more smeared out with first signs of abrasion and deformation. Indications of factory roofs are still present, but change towards the direction of the mode III loading (tangentially). The examined area on the surfaces with higher amounts of mode III torsional loading (specimens (3) and (4), Fig. 7) do not show clear formations of factory roofs, but

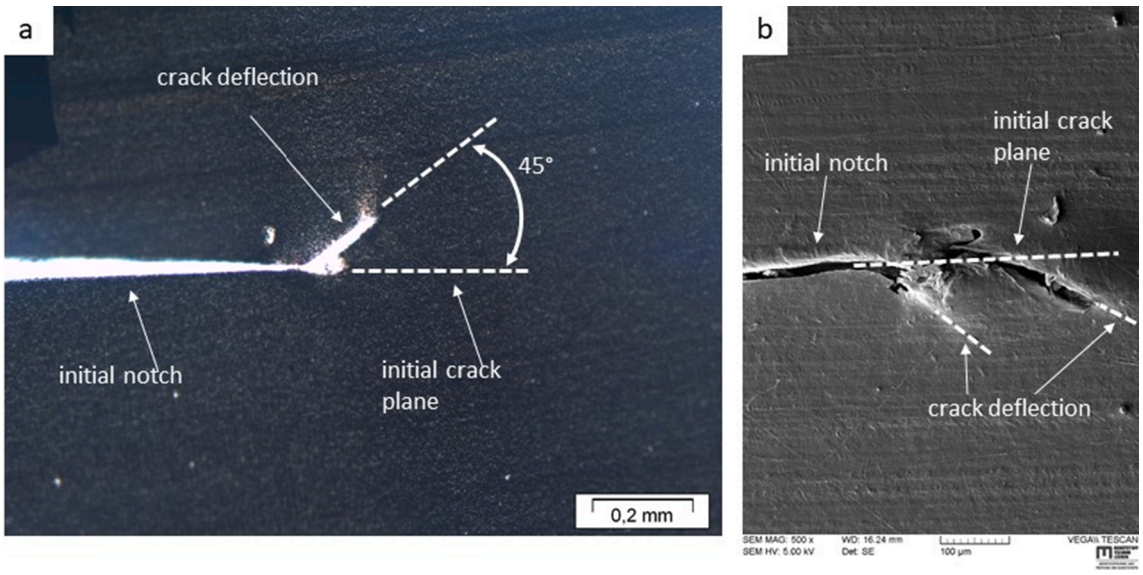

Fig. 8. Crack tip images of mixed mode I/III fatigue loaded PE specimens after the crack freezing experiments showing a branching from the initial crack plane directly after the initial crack tip (analysed using light microscopy (a) and SEM (b, c)).

rather a tangentially deformed texture, which is in agreement with fracture surfaces found on metals [55]. The visible indications of friction and wear abrasion in mode III testing are also supported by the increasing surface temperature measured during fatigue testing (33 °C for specimen 3 and 40 °C for specimen 4). This increase of temperature probably also further accelerates the plastic deformation of the formations on the fracture surface, since mechanical properties of polymers, e. g. the yield strength, are highly sensitive to temperature increases [22,38,39,62].

Interestingly, the governed area of factory roof morphology on the fracture surface seems to be dependent on the applied value of ΔK_{III}. The local stress intensity factor ΔK_{III} at the end of this area had similar values for all investigated specimens, which is shown as the length of the facet-zone l_{facets} in Fig. 6. The change is always accompanied by a local ΔK_{III} value of around 0.9 MPam$^{1/2}$. This indicates that the mode III amount during the experiment increases until a critical value is reached (in this case a ΔK_{III} value of around 0.9 MPam$^{1/2}$), at which point the fracture mechanism changes.

While the formations on the fracture surfaces of specimens with low to moderate levels of ΔK_{III} allow for an interpretation of the fracture mechanism, it is not so clear on the specimens with high amounts of ΔK_{III} due to the smeared-out appearance after testing. To gain more information about the crack growth initiation process of highly deformed mixed mode specimens, like (3) and (4) in Fig. 6, so called crack freezing tests were conducted. Crack freezing experiments provide additional information about the developing crack path and subsequent formation of factory roofs at the beginning of the experiment before they are destroyed by friction and wear abrasion. Therefore, mixed mode I/III experiments were stopped after crack propagation had started but before the significant wear and abrasion, or even final failure occurred. Light-microscope and SEM images of different specimens with similar loading situations to specimen (4) in Fig. 6 (ΔK_I close to 0.7 MPa m$^{1/2}$, ΔK_{III} close to 0.6 MPa m$^{1/2}$) were performed and stopped after around 70 000 cycles. The results of the crack freezing experiments are shown in Fig. 8.

As discussed above, mode III can cause interactions during the tests, such as friction and wear abrasion due to the closed crack flanks, but also mode I branching. The latter phenomenon is a competition between

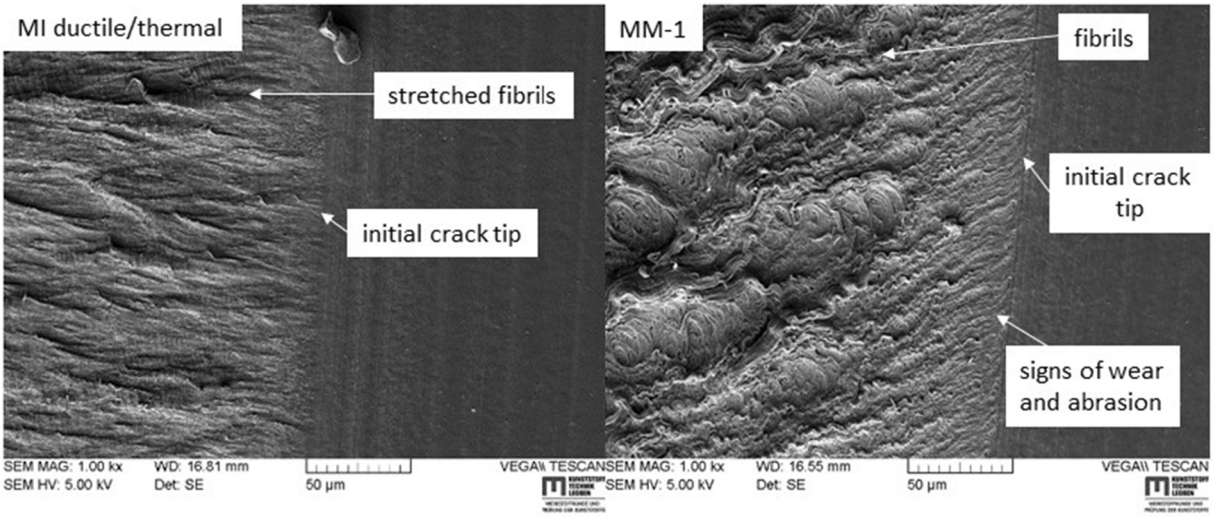

Fig. 9. SEM picture of the area close to the initial crack tip of fatigue loaded PE specimens: highly loaded mode I specimen ("MI ductile/thermal") in comparison with a mixed mode I/III ("MM- 1") specimen with a high level of mode III loading.

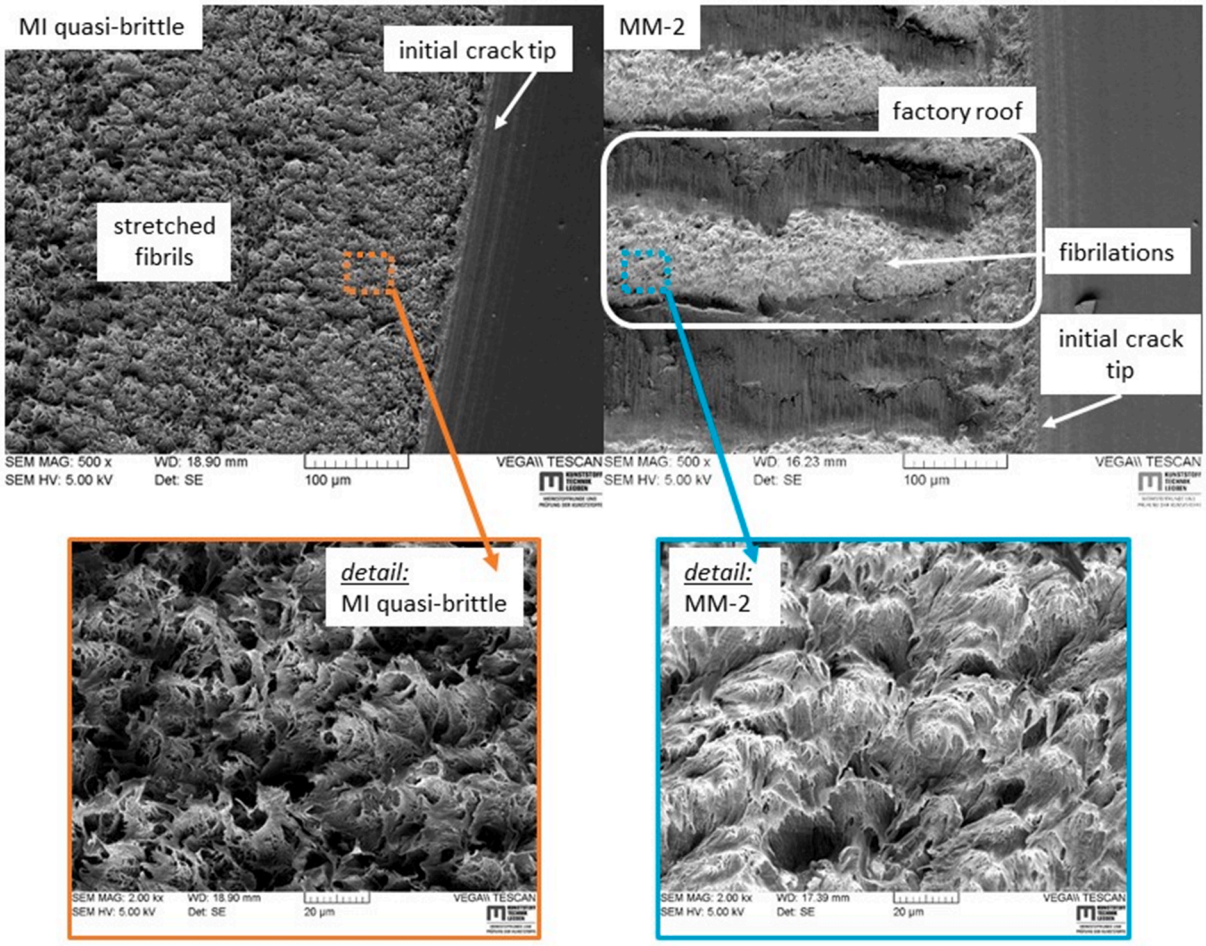

Fig. 10. SEM picture of the area close to the initial crack tip of fatigue loaded PE specimens: moderately loaded mode I specimen ("MI quasi-brittle") in comparison with a mixed mode I/III specimen ("MM- 2" with a low level of mode III loading) and a detailed comparison of the fibrillations.

the shear (mode II and mode III) and tensile (mode I) crack opening modes and leads to crack plane twisting (crack deflection) and subsequent factory roof formations on the fracture surface [8]. Although no clear factory roof formations are visible for specimens (3) and (4) on the fracture surfaces post mortem, the crack-freezing results in Fig. 8 show, that there are deflecting cracks with sloped crack fronts. This was also found for metals under mixed mode I/III loading [7,55,56,63]. The deflection of these cracks is marked in Fig. 8-a, where the light microscope image displays a nearly 45° kink of the crack front immediately after the initial crack tip. This is typically found during the formation of factory roofs. Also in the SEM images (Fig. 8-b), the crack plane rotation after the initial notch plane is clearly visible. In Fig. 8-b, the crack arrests in the first twisted crack before the crack growth continues to the next deflection. The growth happens close to the initial plane. This behaviour supports the appearance of factory roof formations as typical indications for mixed mode I/III crack growth also for highly loaded specimens, before these artefacts are destroyed by friction and wear abrasion.

Finally, after examination of the macro- and microscopic failure behaviour and appearance, it is also important to understand the underlying failure mechanism on a molecular level. As stated in the beginning, PE usually fails by the formation and breakdown of crazes in the quasi-brittle region. Since this area is especially interesting for lifetime estimations later on, it is necessary to investigate the influence of mode III loading with this regard as well.

3.3.3. *Fracture surface - microscopic level*

To examine the mechanisms occurring on the fracture surfaces, SEM pictures were taken from the mode I and mixed mode I/III specimens presented in Fig. 5. Fig. 9 presents the mode I specimen in the region of "MI ductile/thermal" failure in comparison to the mixed mode I/III specimen with a high amount of mode III loading ("MM-1").

The "MI ductile/thermal" fracture surface in Fig. 9 displayed indications of plastic deformation in the form of large stretched fibrils oriented in the direction of crack growth. These stretched fibrils are a sign of plastic surface flow [50,51,53]. The mixed mode I/III loaded specimen with high amounts of mode III presented in Fig. 9 ("MM-1") displayed signs of wear and abrasion close to the initial crack tip, which, as previously stated, is also reflected by the comparatively high specimen surface temperatures measured for this specimen (around 40 °C).

In Fig. 10, SEM images of the area close to the initial crack tip are shown for a mode I quasi-brittle fracture surface ("MI quasi brittle") and for a mixed mode I/III fracture surface with low amounts of mode III loading and suspected "crack closure" ("MM-2").

The crack growth initiation area of the "MI quasi-brittle" specimen in Fig. 10 displays fine fibrillations on the fracture surface, which is an indication of creep and fatigue crack growth in combination with discontinuous crack, as previously discussed for PE [50,53]. The mixed mode I/III fracture surface in Fig. 10 with low amounts of mode III loading ("MM-2") displays two clearly different mechanisms on the opposite side of the factory roofs. On one side of the factory roof also fibrillations, which show a similar appearance compared to pure mode I fibrillations (detail SEM pictures in Fig. 10), can be detected. On the other side of the factory roof the surface structure is more deformed and no fibrillation was observed. An explanation of the difference on the two

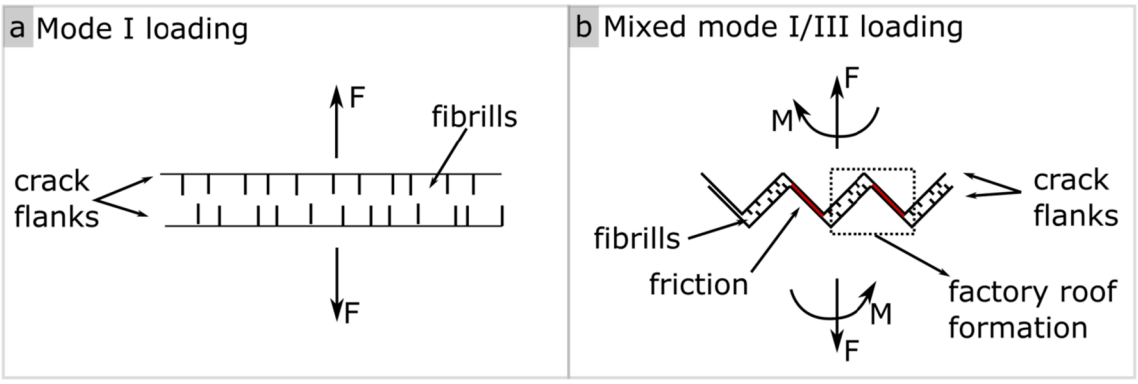

Fig. 11. Schematic illustration of the development of fibrils in pure mode I loading (a) and mixed mode I/III loading, where fibrils are present only on one side of the factory roof formation and friction and wear are supposed for the other side (b).

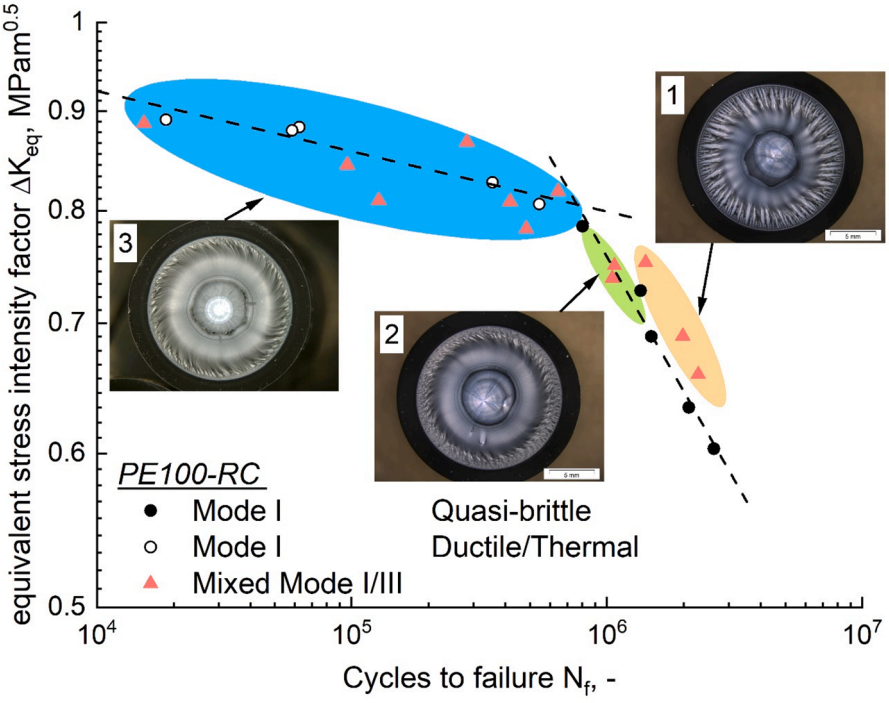

Fig. 12. The fatigue fracture behaviour of PE presented as the equivalent stress intensity factor ΔK_{eq} in pure mode I and mixed mode I/III fatigue testing is influenced by three effects marked as: (1) crack closure effect leads to increasing cycles to failure, (2) mixed mode fracture and (3) thermally induced failure.

sides of the factory roofs is schematically shown in Fig. 11, where pure mode I fibrils are compared to the factory roof formations in mixed mode I/III with fibrils on one side.

From the surface appearance in Fig. 10, it is supposed that the other side of the factory roof is exposed to friction and wear. The occurrence of fibrillation on only one side of the mixed mode facets is explained by the direction of the applied torque for the mode III loading. Since an R-ratio of 0.1 was applied, the specimen was deformed in mode III up to a certain value and afterwards unloaded to 10% of this value. Consequently, it was never completely unloaded or even loaded with a negative torque. Hence, only one side of the factory roof was loaded locally in positive mode I (through the crack plane rotation) and the fibrillations are only visible on this side. On the other side of these mixed-mode facets, wear and abrasion caused a smeared-out structure. However, compared to specimens with high amounts of ΔK_{III}, the measured surface temperature increase was less pronounced. These results are a further indication, that the specimen is locally loaded in mode I due to a twisting of the crack plane. Therefore, the same underlying fracture mechanisms, which ae often summarized as crazing, appear to be driving mechanisms of the failure of the PE material on one side of the factory roofs, while the other side shows clear indications of wear and abrasion.

4. Conclusions

The influence of mixed mode I/III fatigue loading on PE was characterized and compared to pure mode I fatigue results of this material. The aim was to continue the research on mixed mode fatigue loading of

polymers with a comparatively well analysed reference material (PE).

In a first comparison of applied ΔK_I and corresponding failure cycles N_f, the additional loading in mode III led to a significant decrease in the measured life-times compared to pure mode I fatigue experiments. For small amounts of mode III loading a similar slope as for the pure mode I quasi-brittle curve was observed only shifted to a lower life-time. For the comparison of both loading cases, the equivalent stress intensity factor ΔK_{eq} was evaluated, which led to a good correlation of pure mode I and mixed mode I/III experiments was observed. To provide an overview of the effects influencing mixed mode I/III fatigue crack growth in PE, the fatigue fracture curve based on the ΔK_{eq} was plotted again in Fig. 12, and the identified influences are marked as: (1) crack closure effect, (2) mixed mode I/III crack growth and (3) thermally induced failure.

For mixed mode I/III data points with low amounts of mode III (marked as (1) in Fig. 12) a slight increase in the measured cycles to failure was detected. This increasing life-time can be explained by the crack closure effect, where the driving force for crack growth is reduced due to a closed crack tip [8,28,58,59,61]. This is also visible on the investigated fracture surfaces, where characteristic factory roof formations, which are typical for mode III fracture, were observed. Mixed mode I/III specimens from the area (2) marked in Fig. 12, appear to be no longer influenced by crack closure effects and display a good correlation with the resulting ΔK_{eq} of pure mode I data points. Finally, the thermally induced failure (marked as (3) in Fig. 12), which is governed by abrasion between the crack flanks and hysteretic heating, is shown on the left side of the plot. The increasing temperature, friction and wear during testing also significantly alter the fracture surfaces, where a flat and smeared out appearance was detected. This aspect is especially critical for the measured life-time, since polymers are highly sensitive to temperature.

In future research, the results based on the equivalent stress intensity factor K_{eq} have to be compared with life-time simulations to further verify the results of this study. It is also important to expand this research by testing more materials to strengthen the knowledge of mixed mode I/III fatigue loading in plastics. Furthermore, mode II loading tests will be conducted to build a complete understanding for mixed mode crack growth effects in polymers.

Declaration of Competing Interest

The authors declare that they have no known competing financial interests or personal relationships that could have appeared to influence the work reported in this paper.

Acknowledgement

The research work of this paper was performed at the Materials Science and Testing of Polymers/Montanuniversitaet Leoben within the framework of the COMET-program of the Federal Ministry for Transport, Innovation and Technology and the Federal Ministry of Science, Research and Economy with contributions by Polymer Competence Center Leoben GmbH and Institute of Physics of Materials AS CR/Czech Republic.

Appendix A

A.1. Specimen compliance and hysteretic loops

As mentioned in the manuscript, it was not possible to use the specimen compliance for a precise identification of the crack growth initiation or subsequent analysis of crack growth behavior via a compliance calibration. Due to the restrictions of the experimental setup, it is only possible to use the displacement data of the machine actuator. Therefore, the compliance data is too coarse for any detailed analysis of the mixed mode I/III crack growth behaviour. For illustration, the evaluated dynamic specimen compliance ($\Delta C = (displacement_{max} - displacement_{min})/(force_{max} - force_{min})$ during a cycle) from the machine data is shown in Fig. A1 for a mixed mode I/III specimen for both axial and torsional orientation.

Subsequent analysis of the whole load–displacement hysteresis, as shown in Fig. A2 for both regions in the failure curve and Fig. A3 for a mixed mode I/III specimen, did also not allow for further analysis of the crack growth kinetics, or point of crack growth initiation. All hysteresis loops shift towards higher displacements during testing due to creep of the whole specimen. However, a clear change of slope ($=1/\Delta C$) or shape of the hysteresis is only visible in the last few cycles before failure. Only the specimen failing in a ductile/thermal way (Fig. A3 on the right) shows a continuous change due to the steady increase in temperature.

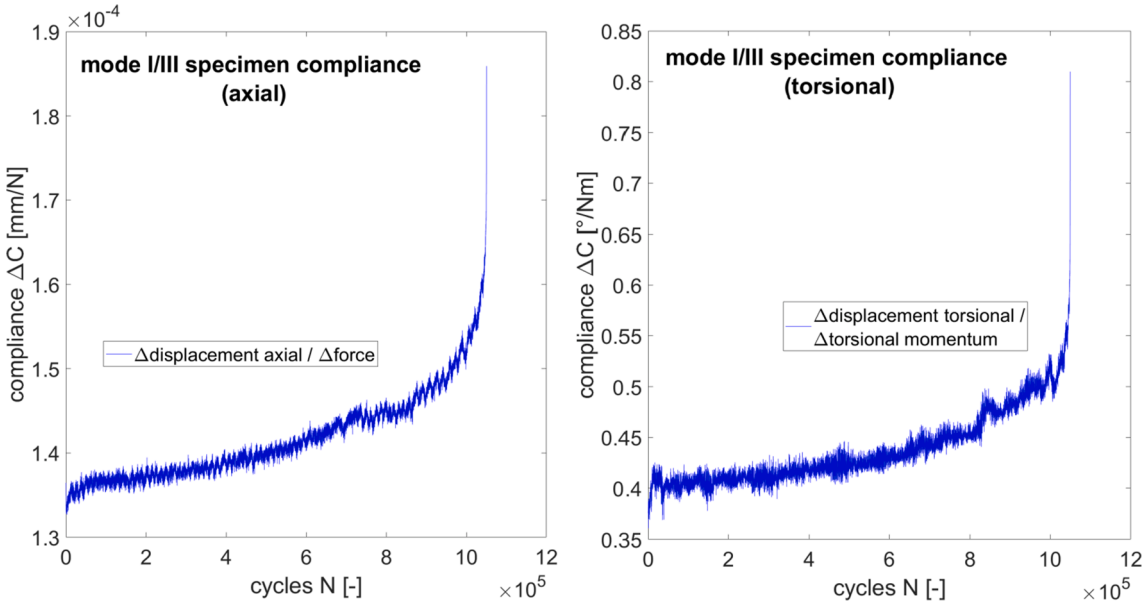

Fig. A1. Cyclic axial and torsional specimen compliance, recorded using the actuator of the testing machine during a mixed mode I/III test without clear indications of crack growth initiation.

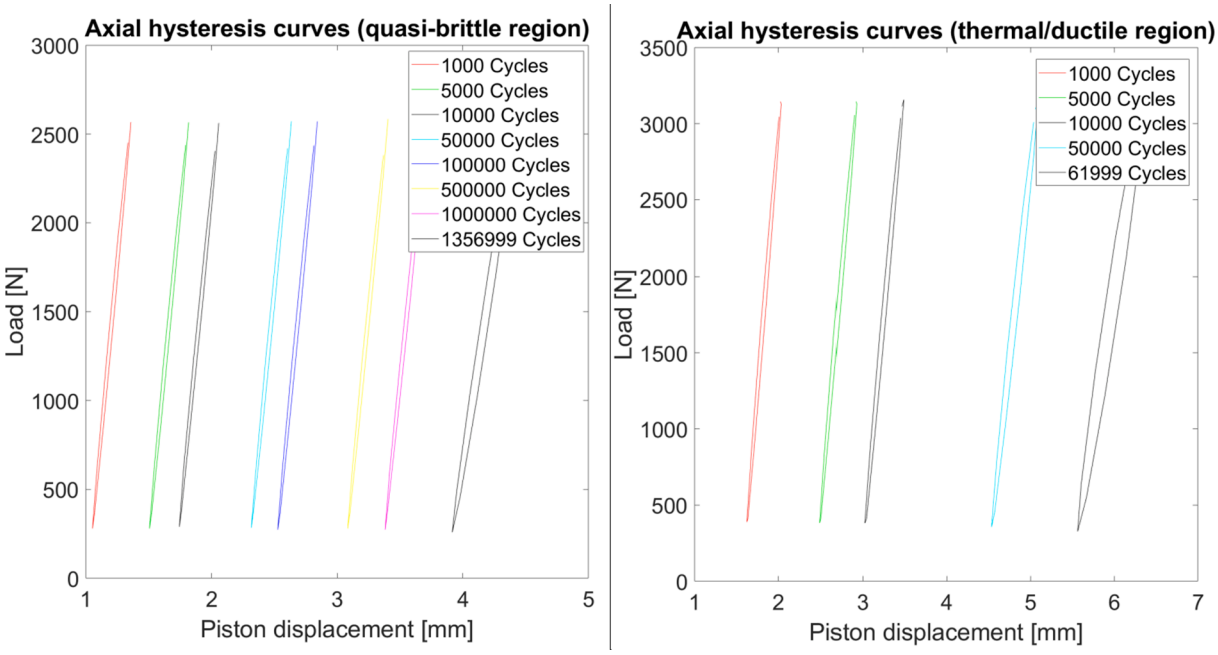

Fig. A2. Axial hysteresis curves in pure mode I loading tested samples in the quasi-brittle region and the thermal/ductile region.

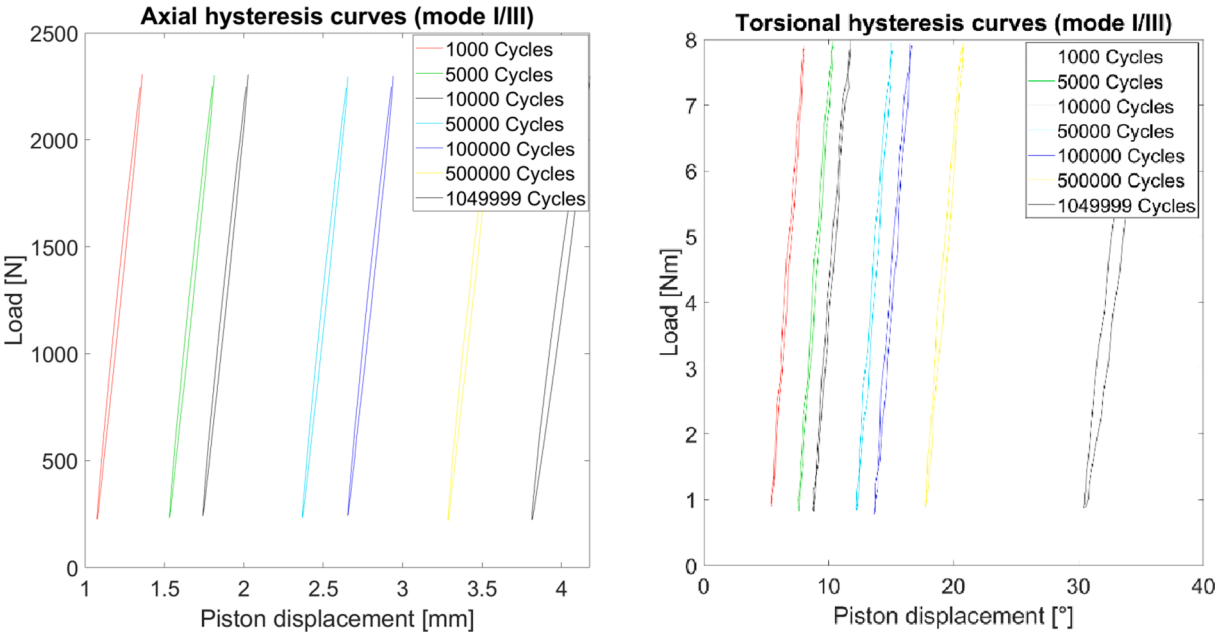

Fig. A3. Axial and torsional hysteresis curves in mixed mode I/III loading.

References

[1] Rösler J. Zur Tragfähigkeitssteigerung thermoplastischer Zahnräder mit Füllstoffen [Dissertation]. Berlin: Technischen Universität Berlin; 2004.

[2] Dlhy P, Poduska J, Nahlik L, Berer M, Gosch A, Pinter G, et al. Compression-loaded cracked cylinder - stress intensity factor evaluation. Key Eng Mater 2018;774:331–6. https://doi.org/10.4028/www.scientific.net/KEM.774.331.

[3] Berer M, Major Z. Characterization of the global deformation behaviour of engineering plastics rolls. Int J Mech Mater Des 2010;6(1):1–9. https://doi.org/10.1007/s10999-010-9111-9.

[4] Berer M, Major Z. Characterisation of the local deformation behaviour of engineering plastics rolls. Strain 2012;48(3):225–34. https://doi.org/10.1111/j.1475-1305.2011.00816.x.

[5] Berer M, Major Z, Pinter G. Elevated pitting wear of injection molded polyetheretherketone (PEEK) rolls. Wear 2013;297(1–2):1052–63. https://doi.org/10.1016/j.wear.2012.11.062.

[6] Slávik O, Hutař P, Gosch A, Berer M, Vojtek T, Arbeiter F, et al. Fatigue crack propagation under mixed Mode I and III in polyoxymethelene homopolymer. Key Eng Mater 2019;827:404–9. https://doi.org/10.4028/www.scientific.net/KEM.827.404.

[7] Beretta S, Foletti S, Valiullin K. Fatigue crack propagation and threshold for shallow micro-cracks under out-of-phase multiaxial loading in a gear steel. Eng Fract Mech 2010;77(11):1835–48. https://doi.org/10.1016/j.engfracmech.2010.05.015.

[8] Vojtek T, Pokluda J, Hohenwarter A, Pippan R. Three-dimensional morphology of fracture surfaces generated by modes II and III fatigue loading in ferrite and austenite. Eng Fract Mech 2013;108:285–93. https://doi.org/10.1016/j.engfracmech.2013.02.022.

[9] Doquet V, Pommier S. Fatigue crack growth under non-proportional mixed mode loading in ferritic pearlitic steel. Fatigue Fract Eng Mater Struct 2004;27:1051–60. https://doi.org/10.1111/j.1460-2695.2004.00817.x.

[10] Qian J, Fatemi A. Mixed mode fatigue crack growth: A literature survey. Eng Fract Mech 1996;55:969–90.

[11] Berer M, Mitev I, Pinter G. Finite element study of mode I crack opening effects in compression-loaded cracked cylinders. Eng Fract Mech 2017;175:1–14. https://doi.org/10.1016/j.engfracmech.2017.03.008.

[12] Gosch A, Berer M, Hutař P, Slávik O, Vojtek T, Arbeiter FJ, et al. Mixed Mode I/III fatigue fracture characterization of Polyoxymethylene. Int J Fatigue 2020;130:105269. https://doi.org/10.1016/j.ijfatigue.2019.105269.

[13] Arbeiter FJ, Frank A, Pinter G. Influence of molecular structure and reinforcement on fatigue behavior of tough polypropylene materials. J Appl Polym Sci 2016;133(38):1237. https://doi.org/10.1002/app.43948.

[14] Pinter G, Haager M, Balika W, Lang RW. Cyclic crack growth tests with CRB specimens for the evaluation of the long-term performance of PE pipe grades. Polym Test 2007;26(2):180–8. https://doi.org/10.1016/j.polymertesting.2006.09.010.

[15] Barker MB, Bowman J, Bevis M. The performance and causes of failure of polyethylene pipes subjected to constant and fluctuating internal pressure loadings. J Mater Sci 1983;18:1095–118.

[16] Lang RW, Stern A, Doerner G. Applicability and limitations of current lifetime prediction models for thermoplastics pipes under internal pressure. Angew Markomol Chem 1997;247:131–45.

[17] Sehanobish K, Moet A, Chudnovsky A, Petro PP. Fractographic analysis of field failure in polyethylene pipe. J Mater Sci 1985;4:890–4.

[18] Lu X, Brown N. A test for slow crack growth failure in Polyethylene under a constant load. Polym Test 1992;11:309–19.

[19] Haager M, Pinter G, Lang RW. Estimation of slow crack growth behavior in polyethylene after stepwise isothermal crystallization. Macromol. Symp. 2004;217(1):383–90. https://doi.org/10.1002/masy.200451334.

[20] Abdel-Bary EM. Handbook of plastic films. UK: Shawbury; 2003.

[21] ISO International Organization for Standardization. Polyethylene (PE) materials for piping systems — Determination of resistance to slow crack growth under cyclic loading — Cracked Round Bar test method(ISO 18489). Switzerland; 2015.

[22] Frank A, Redhead A, Pinter G. The influence of test frequency and eccentric crack growth on cyclic CRB tests. Unpublished; 2012.

[23] Scibetta M, Chaouadi R, Van Walle E. Fracture toughness analysis of circumferentially-cracked round bars. Int J Fract 2000;104:145–68.

[24] Tada H, Paris P, Irwin GR. The stress analysis of cracks. Del Research Corporation; 2003.

[25] Anderson TL. Fracture mechanics: Fundamentals and applications. Taylor & Francis Group, LLC; 2005.

[26] Richard HA, Schramm B, Schirmeisen N-H. Cracks on Mixed Mode loading – Theories, experiments, simulations. Int J Fatigue 2014;62:93–103. https://doi.org/10.1016/j.ijfatigue.2013.06.019.

[27] Tanaka K. Fatigue crack propagation from a crack inclined to the cyclic tensile axis. Eng Fract Mech 1974;6:493–507.

[28] Vojtek T, Pokluda J, Šandera P, Horníková J, Hohenwarter A, Pippan R. Analysis of fatigue crack propagation under mixed mode II+III in ARMCO iron. Int J Fatigue 2015;76:47–52. https://doi.org/10.1016/j.ijfatigue.2014.09.018.

[29] Pokluda J, Pippan R. Can pure mode III fatigue loading contribute to crack propagation in metallic materials? Fatigue Fract Eng Mater Struct 2005;28(1–2):179–85. https://doi.org/10.1111/j.1460-2695.2004.00843.x.

[30] Doquet V, Bui QH, Bertolino G, Merhy E, Alves L. 3D shear-mode fatigue crack growth in maraging steel and Ti-6Al-4V. Int J Fract 2010;165(1):61–76. https://doi.org/10.1007/s10704-010-9504-7.

[31] Frank A, Freimann W, Pinter G, Lang RW. A fracture mechanics concept for the accelerated characterization of creep crack growth in PE-HD pipe grades. Eng Fract Mech 2009;76(18):2780–7. https://doi.org/10.1016/j.engfracmech.2009.06.009.

[32] Frank A, Arbeiter FJ, Berger IJ, Hutař P, Náhlík L, Pinter G. Fracture mechanics lifetime prediction of polyethylene pipes. J Pipeline Syst Eng Pract 2019;10(1):4018030. https://doi.org/10.1061/(ASCE)PS.1949-1204.0000356.

[33] Brown N, Donofrio J, Lu X. The transition between ductile and slowcrack- growth failure in polyethylene. Polymer 1987;28:1326–30.

[34] Gedde UW, Ifwarson M. Molecular structure and morphology of crosslinked polyethylene in an aged hot-water pipe. Polym Eng Sci 1990;30(4):202–10. https://doi.org/10.1002/pen.760300403.

[35] Krishnaswamy RK. Analysis of ductile and brittle failures from creep rupture testing of high-density polyethylene (HDPE) pipes. Polymer 2005;46(25):11664–72. https://doi.org/10.1016/j.polymer.2005.09.084.

[36] Deblieck RAC, van Beek DJM, Remerie K, Ward IM. Failure mechanisms in polyolefines: The role of crazing, shear yielding and the entanglement network. Polymer 2011;52(14):2979–90. https://doi.org/10.1016/j.polymer.2011.03.055.

[37] Lu X, Brown N. Unification of ductile failure and slow crack growth in an ethylene-octene copolymer. J Mater Sci 1991;26(3):612–20. https://doi.org/10.1007/BF00588295.

[38] Lang RW. Applicability of Linear Elastic Fracture Mechanics to Fracture in Polymers and Short-Fiber Composites [Dissertation]: Leigh University; 1984.

[39] Hertzberg RW, Manson JA. Fatigue of engineering plastics. New York, NY: Acad. Press; 1980.

[40] Stern A, Novotny M, Lang RW. Creep crack growth testing of plastics—I. test configurations and test system design. Polym Test 1998;17(6):403–22. https://doi.org/10.1016/S0142-9418(97)00067-6.

[41] Stern A. Fracture mechanical characterization of the long-term behavior of polymers under static loads [Ph.D. Dissertation]. Leoben: Montanuniversitaet; 1995.

[42] Lang RW, Balika W, Pinter G. Applicability of linear elastic fracture mechanics to fatigue in amorphous and semi-crystalline polymers. In: Moore DR, editor. The application of fracture mechanics to polymers, adhesives and composites: European Structural Integrity Society ESIS Technical Comitee 4 (TC4). Elsevier; 2004. p. 83–92.

[43] Barenblatt GI. The mathematical theory of equilibrium cracks in brittle fracture. In: Dryden HL, von Kármán T, Kuerti G, van den Dungen FH, Howarth L, editors. Advances in applied mechanics. Elsevier; 1962. p. 55–129.

[44] Kausch-Blecken von Schmeling H-H. Polymer fracture. Berlin, Heidelberg: Springer; 1978.

[45] Parsons M, Stepanov EV, Hiltner A, Baer E. The damage zone ahead of the arrested crack in polyethylene resins. J Mater Sci 2001;36(24):5747–55. https://doi.org/10.1023/A:1012935517866.

[46] Berer M, Major Z, Pinter G, Constantinescu DM, Marsavina L. Investigation of the dynamic mechanical behavior of polyetheretherketone (PEEK) in the high stress tensile regime. Mech Time-Depend Mater 2014;18:663–84. https://doi.org/10.1007/s11043-013-9211-7.

[47] Berer M, Tscharnuter D, Pinter G. Dynamic mechanical response of polyetheretherketone (PEEK) exposed to cyclic loads in the high stress tensile regime. Int J Fatigue 2015;80:397–405. https://doi.org/10.1016/j.ijfatigue.2015.06.026.

[48] Arbeiter F, Pinter G, Frank A. Characterisation of quasi-brittle fatigue crack growth in pipe grade polypropylene block copolymer. Polym Test 2014;37:186–92. https://doi.org/10.1016/j.polymertesting.2014.05.016.

[49] Favier V, Giroud T, Strijko E, Hiver JM, G'Sell C, Hellinckx S, et al. Slow crack propagation in polyethylene under fatigue at controlled stress intensity. Polymer 2002;43:1375–82.

[50] Hamouda HBH, Simoes-betbeder M, Grillon F, Blouet P, Billon N, Piques R. Creep damage mechanisms in polyethylene gas pipes. Polymer 2001;42:5425–37.

[51] Parsons M, Stepanov EV, Hiltner A, Baer E. Correlation of fatigue and creep slow crack growth in a medium density polyethylene pipe material. J Mater Sci 2000;35:2659–74.

[52] Pinter G, Lang RW. Creep crack growth in high density polyethylene. In: Moore DR, editor. The application of fracture mechanics to polymers, adhesives and composites: European Structural Integrity Society ESIS Technical Comitee 4 (TC4). Elsevier; 2004. p. 47–54.

[53] Arbeiter F, Schrittesser B, Frank A, Berer M, Pinter G. Cyclic tests on cracked round bars as a quick tool to assess the long term behaviour of thermoplastics and elastomers. Polym Test 2015;45:83–92. https://doi.org/10.1016/j.polymertesting.2015.05.008.

[54] Nayeb-Hashemi H, McClintock FA, Ritchie RO. Effects of friction and high torque on fatigue crack propagation in Mode III. MTA 1982;13(12):2197–204. https://doi.org/10.1007/BF02648390.

[55] Tschegg EK. Mode III and Mode I fatigue crack propagation behaviour under torsional loading. J Mater Sci 1983;18:1604–14.

[56] Tschegg EK, Ritchie RO, McClintock FA. On the influence of rubbing fracture surfaces on fatigue crack propagation in Mode III. Int J Fatigue 1983:29–35.

[57] Tschegg FK. Sliding mode crack closure and Mode III fatigue crack growth in mild Steel. Acta Metall 1983;9:1323–30.

[58] Pippan R, Hohenwarter A. Fatigue crack closure: a review of the physical phenomena. Fatigue Fract Eng Mater Struct 2017;40(4):471–95. https://doi.org/10.1111/ffe.12578.

[59] Suresh S, Ritchie RO. A geometric model for fatigue crack closure induced by fracture surface roughness. MTA 1982:13A.

[60] Vojtek T, Pippan R, Hohenwarter A, Holan L, Pokluda J. Near-threshold propagation of mode II and mode III fatigue cracks in ferrite and austenite. Acta Mater 2013;61:4325–635. https://doi.org/10.1016/j.actamat.2013.04.033.

[61] Pokluda J, Pippan R, Vojtek T, Hohenwarter A. Near-threshold behaviour of shear-mode fatigue cracks in metallic materials. Fatigue Fract Eng Mater Struct 2013;37:232–54. https://doi.org/10.1111/ffe.12131.

[62] Hertzberg RW, Vinci RP, Hertzberg JL. Deformation and fracture mechanics of engineering materials. 5th ed. Hoboken, NJ: Wiley; 2013.

[63] Zhizhong H, Lihua M, Shuzhen C. A study of shear fatigue crack mechanisms. Fatigue Fract Eng Mater Struct 1992;15(6):563–72.